



**HAL**  
open science

# Graphene quantum dots: Emerging organic materials with remarkable and tunable luminescence features

Philippe Pierrat, Jean-Jacques Gaumet

► **To cite this version:**

Philippe Pierrat, Jean-Jacques Gaumet. Graphene quantum dots: Emerging organic materials with remarkable and tunable luminescence features. *Tetrahedron Letters*, 2020, 61 (49), pp.152554. 10.1016/j.tetlet.2020.152554 . hal-03016684

**HAL Id: hal-03016684**

**<https://hal.univ-lorraine.fr/hal-03016684>**

Submitted on 21 Nov 2022

**HAL** is a multi-disciplinary open access archive for the deposit and dissemination of scientific research documents, whether they are published or not. The documents may come from teaching and research institutions in France or abroad, or from public or private research centers.

L'archive ouverte pluridisciplinaire **HAL**, est destinée au dépôt et à la diffusion de documents scientifiques de niveau recherche, publiés ou non, émanant des établissements d'enseignement et de recherche français ou étrangers, des laboratoires publics ou privés.



Distributed under a Creative Commons Attribution - NonCommercial 4.0 International License



## Graphene Quantum Dots: Emerging Organic Materials with Remarkable and Tunable Luminescence Features

Philippe Pierrat<sup>a,\*</sup> and Jean-Jacques Gaumet<sup>b</sup>

<sup>a</sup>Université de Lorraine, CNRS, L2CM, F-57000, Metz, France

<sup>b</sup>Université de Lorraine, LCP-A2MC, EA4632, Institut Jean Barriol, F-57070, Metz, France

### ARTICLE INFO

#### Article history:

Received

Received in revised form

Accepted

Available online

#### Keywords:

Keyword\_1 Graphene quantum dot

Keyword\_2 Fluorescence

Keyword\_3 Phosphorescence

Keyword\_4 Polycyclic aromatic hydrocarbons

Keyword\_5 Nanoparticles

### ABSTRACT

Graphene quantum dots (GQDs) are recently discovered carbon-based materials that correspond to nano-fragments of functional graphene-like structures. They could be synthesized either by conventional stepwise organic synthesis or, more rapidly, by either top-down or bottom-up one step approaches. Regardless of the synthetic route, GQDs display photoluminescence features (fluorescence and/or phosphorescence) that could be finely tuned according to their surface and edges chemistry. This makes this new organic material highly valuable in applications ranging from imaging, sensing and optoelectronics.

2009 Elsevier Ltd. All rights reserved.

Graphene corresponds to an infinite 2D monolayer of hexagonal  $sp^2$  bonded carbon network which shows interesting properties of zero band gap due to the delocalized electrons. Consequently this gives a semi-metallic behavior to graphene and as a consequence electrons move through with virtually no resistance leading to high electrical conductivity. Owing to other remarkable properties such as strength, lightness, thermal conductivity and transparency, graphene holds great promise in semiconductors, electronic and energy storage applications. Nevertheless, large scale production of high quality graphene together with its low processability still constitute key technical hurdles to overcome in order to allow graphene to reach industry scale-up. Moreover, it is still a critical challenge to set up stable and homogeneous dispersions of graphene without agglomeration. Furthermore, the zero bandgap of graphene hampers their implementation in optoelectronic devices as well as in field-effect transistors (FETs). In that context, the recent discovery of graphene quantum dots (GQDs) and the rapid advances in their synthetic preparation do offer a unique opportunity for investigating their applications as potential highly soluble graphene-based substitutes and displaying tunable bandgap owing to either quantum confinement effect or heteroatom doping or both phenomena.<sup>1</sup> These carbonaceous quantum dots combine several favorable attributes of traditional semiconductor-based quantum dots (namely, nanoscale size, size- and wavelength-dependent luminescence emission, resistance to photobleaching, ease of bioconjugation) without incurring the burden of intrinsic toxicity or elemental scarcity, and without the need for stringent, costly, or inefficient preparation steps.

GQDs are functionalized nanofragments of graphene with lateral size generally below 10 nm. Their anisotropic morphology

originates from lateral dimension that is larger than their height. GQDs systematically possess graphitic lattices within their structures, as evidenced by high-resolution transmission electron microscopy (HR-TEM). Their height is usually ranging from 0.4 to 4 nm as evidenced by statistical AFM analysis, which corresponds to few GQDs (from 1 to 10) stacked on the top of each other. GQDs could be merely considered as polycyclic aromatic hydrocarbons (PAHs) "molecules" larger than 1 nm. Multistep organic synthesis of GQDs is highly challenging, usually involving many successive chemical transformations from a commercially available chemical. As GQDs are composed of many fused aromatics, their synthesis usually involved one or many key annulation steps. Although hardly transferable at the industrial scale, this stepwise approach has the noteworthy advantage to yield atomically precise nanographene structures, in terms of size and heteroatom doping (heteroatom nature, position and concentration). On the other hand, chemists have also developed GQDs synthetic approaches (either bottom-up or top-down method), in most cases in one step, which end in the preparation of a mixture of GQDs having statistical size and chemistry distribution. Consequently, macroscopic properties arise from those of the total GQDs population.

As mentioned above, stepwise and well-controlled organic synthesis of GQDs is a highly challenging task which allows to set reliable structure-properties relationships. It relies on multi-step synthesis associated with tedious purification at each step (most often by standard column chromatography), which limits therefore the potential of this approaches to be easily scaled-up. In that case, accurate characterization of the products involve classical NMR spectroscopy and mass spectrometry. For instance, Müllen's group developed the synthesis of substituted

hexa-*peri*-hexabenzocoronene (HBC) with the key annulation step which was done through a cyclodehydrogenation of the polyphenylene precursors (obtained in 5 steps) using a mixture of  $\text{Cu}(\text{CF}_3\text{SO}_3)_2$  and  $\text{AlCl}_3$  (Figure 1, molecule 1).<sup>2</sup> This methodology has inspired a lot of recent research developments to prepare various heteroatom-doped HBC derivatives which could be considered as N- or S-doped GQDs of precise chemical structure (Figure 1, molecule 2 and 3 and many others).<sup>3,4</sup>

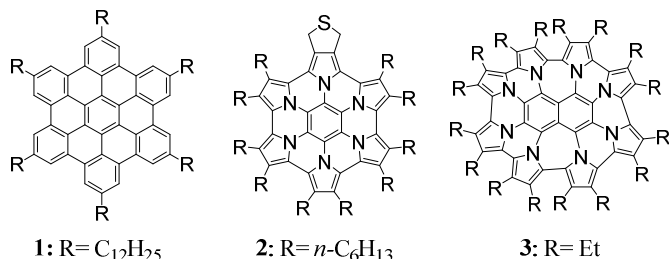
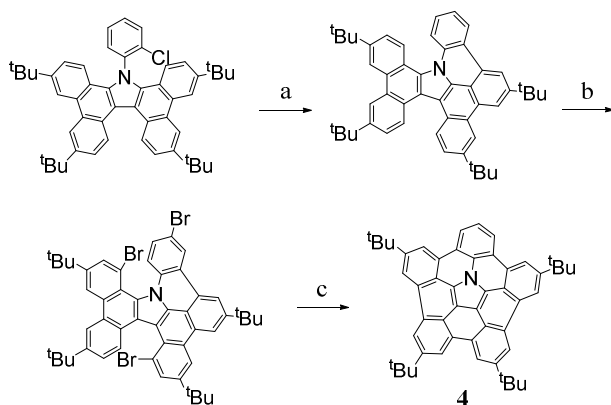


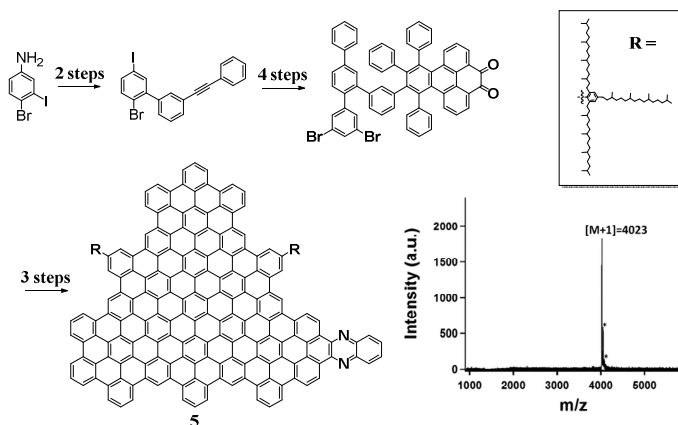
**Figure 1.** Examples of HBC and heteroatom-doped HBC derivatives.

Annulations could also be done under a dehydrohalogenative step through metal-catalyzed Heck-like reactions on already sophisticated organic compounds (Scheme 1).<sup>5</sup>



**Scheme 1.** Synthetic route to N-doped GQD 4. (a)  $\text{Pd}(\text{OAc})_2$ ,  $\text{PCy}_3$ ,  $\text{HBF}_4$ ,  $\text{K}_2\text{CO}_3$ , DMA, 130 °C, 43 h, 63% yield. (b)  $\text{Br}_2$ ,  $\text{CCl}_4$ , 70 °C, 12.5 h, 56% yield. (c)  $\text{Pd}(\text{OAc})_2$ ,  $\text{PCy}_3$ ,  $\text{HBF}_4$ ,  $\text{K}_2\text{CO}_3$ , DMA, 130 °C, 16 h, 46% yield.

Other annulation approaches could rely on Pictet-Spengler reaction,<sup>6</sup> Friedel-Crafts condensation and UV-light irradiation.<sup>7</sup>



**Scheme 2.** Synthetic route to N-doped GQDs 5 with its MALDI-TOF MS spectra. Adapted with permission from reference 8. Copyright (2012) American Chemical Society.

In this context, Li and coworkers have reported on the stepwise synthesis of N-doped graphene quantum dot 5 composed of 67 aromatic rings with interesting electrocatalytic

activity for the oxygen reduction reaction (ORR), starting from 4-bromo-3-iodoaniline in 9 steps (scheme 2).<sup>9</sup> Long alkyl chains were introduced on N-GQDs to ensure their solubility. The defined chemical structure has been confirmed with isotope-resolved MALDI-mass spectrometry for the  $[\text{M}+\text{H}]^+$  at  $m/z$  4023 showing excellent size uniformity.

Above-mentioned examples are some of the many reported developments dealing with the “total” synthesis of accurate chemical structures that could accommodate the definition of GQDs providing standard molecules for studying specific properties. We invite readers interested in further examples to consult selected reviews which give an overview of the synthetic possibilities toward the access to large polycyclic aromatic structures.<sup>10,11</sup>

GQDs can also be produced under straightforward one-step processes which could be classified in two distinct categories and thus rely either on top-down or bottom-up synthetic approaches. This has been the subject of many comprehensive reviews.<sup>12,13</sup> In that context, GQDs are generally purified by dialysis and to a lesser extent by ultracentrifugation or column chromatography. Their characterization rely on material science techniques that are Raman spectroscopy, X-ray photoelectron spectroscopy (XPS), IR-spectroscopy, high resolution transmission electron microscopy (HR-TEM), atomic force microscopy (AFM) and very sparingly dynamic light scattering (DLS) and sometimes mass spectrometry (MS). Briefly, the top-down synthesis deals with chemical breakdown of large carbon-based materials (carbon fibers,<sup>14</sup> graphene oxide GO,<sup>15</sup> coal,<sup>16</sup> fullerenes,<sup>17</sup> graphite,<sup>18</sup>...) into small fragments with concentrated acids. GO is typically the ideal starting material according to the presence of many oxygen-containing functional groups which facilitate the chemical cleavage toward nanosized GQDs. Nevertheless, GO does not naturally occur and has thus to be prepared from various materials such as coal or anthracite by the complex Hummer’s chemical approach. In that context, the use of graphite as natural source has been evaluated as GO substitute with lesser success to date according to lower synthetic yields. Top-down syntheses are reported to be possible through hydrothermal or solvothermal cutting,<sup>19</sup> microwave-assisted exfoliation,<sup>20</sup> electrochemical methods<sup>21</sup> and oxidation.<sup>22</sup> On the other hand, one-step bottom-up synthesis deals with the carbonization of organic precursors (citric acid,<sup>23</sup> glucose,<sup>24</sup> glutamic acid,<sup>25</sup> hexa-*peri*-hexabenzocoronene,<sup>26</sup> ...) by microwave-assisted pyrolysis, solvothermal heating or under pulsed laser irradiation. However, bottom-up approaches generally suffer from lower yields associated with purification hurdles to remove unreacted small organic materials.

GQDs are emerging large organic molecules or nanoparticles (depending on a structural and size point of view) which display very interesting tunable luminescence features opening the door to imaging and sensing applications. Luminescence corresponds to a general mechanism in which a molecule or a material, in an electronically excited state, emits light. This phenomenon, when promoted by an incident light, can be divided into two distinct categories, *i.e.* fluorescence and phosphorescence. Fluorescence emission rates are typically  $\sim 10^8 \text{ s}^{-1}$  while phosphorescence emission rates are in the range of  $10^3$  to  $10^5 \text{ s}^{-1}$ . The main difference between these two phenomena lies in the excited state nature. In case of fluorescence, the excited state corresponds to the presence of an electron in an orbital of higher energy (LUMO) that will naturally pair back with a second electron in the ground state in a rapid manner. In case of phosphorescence, the excited-electron pathway is more complex with an unusual intersystem crossing (ISC) toward a triplet state (*vide infra*).

Carbon dots usually display a bright blue photoluminescent emission peak in the range of 440-580 nm, when excited at 350-400 nm. Their quantum yield (QY) strongly depends on the fabrication method and the surface chemistry involved and usually ranges from a few percent up to 80 % for recent hydrothermal and microwave-assisted fabrication reports. A literature survey shows that most of the reported GQDs display excitation-dependent photoluminescence (PL) features. Interestingly, their fluorescence color could be tuned according to the excitation wavelength, following the general trend that fluorescence color could be red-shifted with decreased excitation energy, nevertheless with emission of gradually weaker intensity. This is so far the only material capable of emitting light of different colors, opening the door to even more potential applications with imaging at the front line. Modulation of the luminescence wavelength could be also achieved by modifying the chemical composition (heteroatom doping<sup>27,28</sup> or passivation strategies using chemical modifications such as introducing PEG chains of various length).<sup>29,30</sup> Since these materials have only recently emerged in the literature, the origins of their PL are still not entirely understood in spite of lot of recent comprehensive studies. At the early stage, the photoluminescence mechanism was attributed to quantum confinement effect (similar to II-VI nanocrystals), nevertheless, this theory is not applicable to graphene-based microstructures.<sup>31</sup> Intensive efforts have thus been devoted to elucidate photoluminescence mechanism through many comprehensive studies in which authors have correlated photophysical features of various carbon-based nanomaterials with morphology, chemical composition with the help of calculations. It is now generally accepted that emission arises from two types of energy states: intrinsic states (band-gap related) formed by isolated polyaromatic structures and extrinsic states (surface related) corresponding to energy states from heteroatoms-based functional groups.<sup>32,33</sup>

Zhu *et al.* investigated thoroughly the impact of the nature of functional groups on PL of GQDs.<sup>34</sup> They demonstrated that starting from GQDs containing -COOH, -OH, epoxy and -NO<sub>2</sub> functional groups, different chemical modifications can be performed inducing PL changes. Carboxyl groups were transformed to amides CON(CH<sub>3</sub>)<sub>2</sub> through a solvothermal treatment in DMF leading to a blue-shifted emission and higher PL intensity. Interestingly, PL intensity and quantum yield could be enhanced by transforming chemical groups which are responsible of non-radiative recombination processes: epoxy groups could be partly transformed to hydroxyl groups under NaBH<sub>4</sub> reduction while high-power UV exposure tends to destroy nitro groups and convert hydroxyl to carbonyl groups. For many applications including optoelectronic applications, it is strongly needed to get unoxidized sp<sup>2</sup> surfaces. In that context, GQDs reduction could also be performed by reacting with hydrazine hydrate.<sup>35</sup> This chemical modification generally allows a high increase of the PL quantum yield by repairing conjugated sp<sup>2</sup> surfaces, forming a pyrazole ring at the platelet edges as well as removing epoxide groups at the GQDs surface. Jang *et al.* focused their attention on elucidating the role of epoxide groups on GQDs photoluminescence.<sup>36</sup> Using a mild and selective epoxide ring opening reaction using oleylamine (OLA) as reagent, different passivated OLA-GQDs were obtained. Combining optical characterizations with DFT calculations allow the authors to demonstrate that epoxide groups are responsible of creating localized sp<sup>2</sup> carbon subdomains, leading to intrinsic fluorescence mostly centered at 400 nm. Graphene quantum dots surface passivation is also considered as an efficient chemical tool to modify PL properties. In that context, Gao *et al.* recently demonstrated that starting from yellow-emitting bare GQDs,

blue- and red-emitting GQDs could be obtained by coating with nitrogen-containing polyethyleneimine (PEI) polymer of different molecular weight (1800 and 600, respectively).<sup>29</sup> Fluorescence wavelength and its pH dependence is strongly correlated with the presence of carboxylic functional groups which, under carboxylate form, are conjugated to the sp<sup>2</sup> structure. Transforming the later in amides with PEI<sub>1800</sub> as amine source leads to a decrease of the edge defect states impact while increasing the intrinsic states emission. As a result, the PL peak was blue-shifted from 510 to 435 nm and the emission color was changed from yellow to blue. When short PEI<sub>600</sub> were used, same chemical modifications occurred, nevertheless, it results in shorter distance between each GQD leading to  $\pi$ -stacked structures in which electrons can move through GQD neighbors. Higher electron delocalization is thus responsible for a shorter band gap and as a result of a red shift in PL emission.

It is now well-recognized that fluorescence of GQDs originates from both the size of sp<sup>2</sup> domain as well as from the nature of functional groups that are located whether at the surface or the edges. However, it is often difficult to distinguish the contribution of each of these mechanisms since one-step synthetic approaches lead to inhomogeneous heteroatom distributions and vacancy defects on GQDs with size distribution of various bandwidth. In order to overcome this difficulty, Yel *et al.* reported on a strategy to produce high-crystallinity, high-uniformity GQDs by fractioning a GQDs batch through successive particle sieving (with polyethersulfone membranes of different pore sizes) in order to elucidate how quantum confinement affect PL emissions.<sup>37</sup>

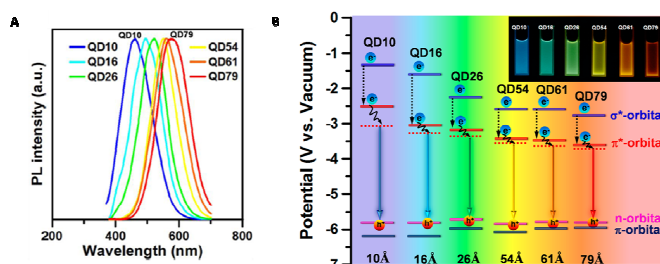


**Figure 2.** (A) Normalized PL spectra of GQDs excited at 350 nm. (B) Schematic energy level diagram for GQD specimens. The PL color varies from orange-red (for QD79) to blue (for QD10). Photographs of aqueous dispersions of GQDs dispersions under UV lamp irradiation (365 nm center wavelength). Adapted with permission from reference 37. Copyright (2016) American Chemical Society.

The authors were able to separate GQDs with size ranging from 1.0 to 7.9 nm having identical chemical functional groups and vacancy defects (Figure 2: from QD10 to QD79, respectively). Thus, since oxygen n-state energy levels are independent of the size of the nanodots, emission wavelength is only dependent on the  $\pi^*$ -n gap which relies only on the sp<sup>2</sup>-domain size. Larger sp<sup>2</sup> domains are thus observed in GQDs of increasing size, leading to  $\pi^*$ -n gap of lower energy, as observed in the photoluminescence spectra. It is noteworthy that all GQDs display excitation-wavelength-independent photoluminescence feature. This illustrates clearly the quantum confinement effect in GQDs with various luminescence. Very recently, Lyu and co-workers report on an elegant, efficient, flexible and scalable approach to prepare GQDs of various PL properties (figure 3).<sup>38</sup> Graphene oxides are first chemically transformed to GQDs in 60% yield through an advanced oxidation process using FeCl<sub>3</sub> and H<sub>2</sub>O<sub>2</sub>. The author's further reported that GQDs of tunable PL feature (blue to red emission) can be simply elaborated when functionalizing parent GQDs with various amines (*e.g.* *m*-phenylenediamine, ethylenediamine...) under a hydrothermal

heating. Conjugating various aromatic amines to GQDs can effectively expand the  $\pi$ -conjugated  $sp^2$  domain, decreasing the LUMO ( $\pi^*$ ) level and thus narrowing the band gap. According to the above-described examples, the photoluminescence of GQDs can be tuned for selected application with the help of chemical tools to modify the surface chemistry.

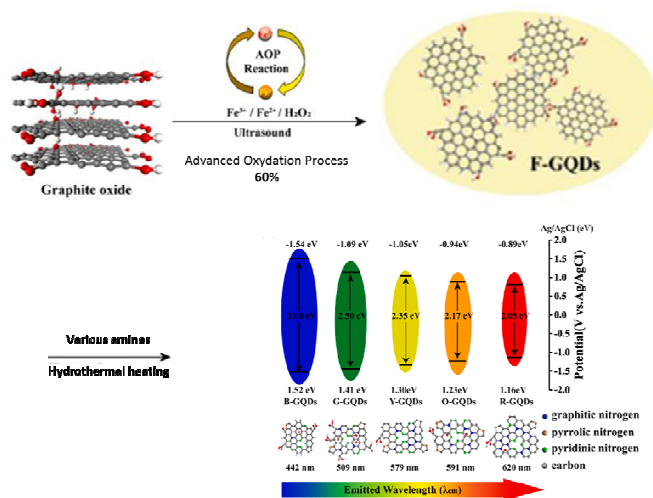


**Figure 3.** Chemical route to prepare GQDs of various emitting color from graphite oxide. Adapted with permission from reference 38. Copyright 2020 Elsevier.

A specific property of GQDs, more particularly the ones with high nitrogen content, is their multi-photon up-conversion photoluminescence (UCPL). UCPL process allows excitation through the simultaneous absorption of two photons of half the energy classically required for the transition, typically in the NIR spectral region, which has a potential for research activities for *in vivo* imaging.<sup>39</sup> Multiphoton imaging allows deeper imaging as well as precise 3D localization in tissues and animals. In that context, GQDs are a potential alternative to semiconductor quantum dots, without displaying avoiding blinking phenomenon with a better biocompatibility. This property offers a lot of potential biomedical applications from diagnosis, imaging and sensing.<sup>40,41</sup>

White-light emissive materials possess a great potential for their uses in optoelectronic devices. In that context, Sekiya *et al.* developed a chemical route to get access to white-light emitting GQDs, by modifying the edge functional groups of GQDs with high quality  $sp^2$  surfaces by incorporating bulky Fréchet's dendritic wedges through a copper-catalyzed Huisgen cycloaddition.<sup>42</sup> In a more recent attempt, Gosh et Prasad demonstrated that white-light emission originates from aggregation of GQDs in solution with CIE (Commission International de l'Éclairage) 1931 chromaticity coordinate ( $x$ ,  $y$ ) values of (0.29, 0.34) is remarkably very close to those of pure white-light emission (0.33, 0.33).<sup>43</sup> Very recent contributions dealing with bright white-light emissive GQDs-based materials showed that GQDs of high PL quantum yields can be prepared by solvothermal heating of 1,5-diaminonaphthalene in  $CHCl_3$ . Interestingly, the mechanochemical grinding of graphite in the presence of melamine (as nitrogen dopant source) and subsequent treatment of the grinded graphite with NaOH allows the introduction of large amount of hydroxyl groups on the graphene layers.<sup>44,45</sup>

Since their discovery, GQDs have been extensively studied for their fluorescence properties and their potential applications. However, to date, only few papers have been published related to

GQDs displaying phosphorescence features. This area of research is still in the early stages. There is a big challenge to develop room temperature phosphorescence (RTP) for technologies including bio-imaging (theranostic agents for backgroundless bio-imaging), photodynamic therapy, organic light-emitting diodes and security applications. Phosphorescence originates from the decay of excitons in the triplet states which are generally spin-forbidden and most of the time wasted under non-radiative relaxation processes such as heat or kinetic energy. Under appropriate excitation wavelength (mostly in the UV region), electrons go from ground state  $S_0$  to excited state  $S_n$  (Figure 4, A). After falling to the  $S_1$  level by internal conversion, luminescence can occur either by fluorescence or by phosphorescence after the  $T_1$  state becomes populated. When the energy gap between  $S_1$  and  $T_1$  ( $\Delta E_{ST}$ ) is appropriate, inter-system crossing becomes possible and electrons may jump from  $S_1$  to  $T_1$ . If  $T_1$  state is not quenched by oxygen or by intramolecular motions, phosphorescence of different colors (according to the  $T_1$ - $S_0$  energy gap) may occur.

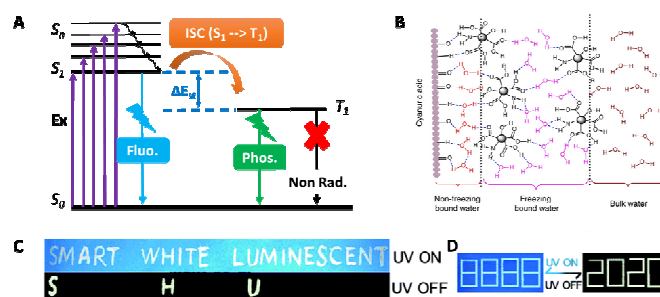


**Figure 4.** (A) Energy-level diagram of the relevant photophysical processes ( $S_0$  = ground state,  $S_1$  = singlet excited state,  $T_1$  = triplet excited state, Fluor. = fluorescence; Phos. = phosphorescence; ISC = intersystem crossing; Ex = excitation; Non Rad. = non radiative). (B) Schematic illustration of the molecular interactions between the GQDs, cyanuric acid particles and water molecules. Adapted with permission from reference 46. Copyright © 2018 Springer Nature. (C-D) Photographs of white-GQDs in information encryption application. (C) “smart white luminescent” is visible under 365 nm UV illumination. Once the lamp is turned off, “SHU” (Shorthand of Shanghai University) of the white color is revealed as a result of the intrinsic emission differences between PL and phosphorescence. (D) The encryption information printed on paper is not identified either under daylight (it was nearly colorless nature of the inks) or under a UV lamp (it showed the wrong information with a white pattern of “8888”). When switching off the excitation, the correct information (“2020”) in white color can be seen clearly. Adapted with permission from reference 47. Copyright (2020) Royal Society of Chemistry.

Most of the phosphorescent materials generally originate from inorganics or metal complexes which are generally unstable, expensive and sometimes toxic. In that context, the development of pure organic compounds showing RTP is highly appealing. Inter-system crossing towards triplet state is usually not observed in pure organic compounds, however, it was demonstrated in 2010 that such mechanism could be observed in graphene quantum dots systems.<sup>48</sup> As GQDs can be assimilated to very large polycyclic aromatic hydrocarbons (PAHs), the singlet-triplet splitting is considerably reduced owing to high electron delocalization which ends in a high probability of inter-system crossing. It has been shown that GQDs could display RTP when they are embedded in host matrices. Such dual system contributes to enhance the spin-orbit coupling of excitons, decrease the singlet-triplet state energy gap, and limit the non-radiative relaxation processes. Either organic or inorganic matrixes have been reported in literature so far. In a seminal paper in 2013,

Deng *et al.* observed RTP in GQDs incorporated within a poly-(vinyl alcohol) PVA matrix, with a phosphorescence lifetime of 380 ms.<sup>49</sup> Since then, a wide range of matrixes has been reported to promote RTP feature such as aluminum sulfate,<sup>50</sup> layer double hydroxides,<sup>51</sup> and calcium carbonate.<sup>52</sup> For instance, the large amount of hydroxyl groups in PVA matrix induces the formation of many hydrogen bonds with carbonyl functions (C=O bonds) on GQDs, limiting intramolecular motion and limiting thus non-radiative deactivation pathways. Li *et al.* demonstrated that high phosphorescence lifetime of 687 ms could be obtained through strong hydrogen bonding of GQDs with a cyanuric acid matrix in presence of water molecules owing to strong hydrogen bonding (Figure 4, B).<sup>46</sup> Long *et al.* recently reported on the synthesis of novel fluorine and nitrogen co-doped GQDs via a one-step solvothermal reaction between glucose and Et<sub>3</sub>N<sub>3</sub>HF.<sup>53</sup> This remarkable new F/N co-doped GQDs constitutes one of the first example of GQDs displaying room temperature phosphorescence with a sub second lifetime (up to 1.2 s under  $\lambda_{exc.} = 260$  nm). Intra/inter dots hydrogen bonds as well as steric protection of C-F bonds contribute to reduce the quenching of RTP by oxygen (forming <sup>1</sup>O<sub>2</sub>) and stabilize the triplet excitons at room temperature. It was very recently reported that phosphorescence of GQDs could also be induced at the solid state upon aggregation<sup>54,55</sup> and that white light phosphorescence, which was not reported so far, could also be observed in single-crystalline chlorinated graphene quantum dots.<sup>47</sup> Over most of the above-cited papers, authors brought out the phosphorescence origin in GQDs. By comparing absorbance spectra with their phosphorescence excitation spectra, there is strong evidence that phosphorescence comes from the n- $\pi^*$  electron transitions of C-N/C=N/C=O/P-N/P=O bonds. RT-phosphorescent GQDs are expected to be new versatile materials to be used in the fight against counterfeiting tag since it consists on cheap and environmental friendly materials that could be nevertheless difficult to reproduce both in terms of synthesis and of phosphorescence lifetime.

To conclude, graphene quantum dots should be regarded as a fascinating recently discovered allotropic carbon form. GQDs may be used as potential graphene substitute, with synthetic methodologies performed either by following standard multistep organic synthesis or by simple one step top-down or bottom-up approaches. Nevertheless, with regard to their wide range of potential applications, particularly the one related to their outstanding luminescence features that are highlighted in this paper, it becomes necessary to develop efficient large production of GQDs to attain an industrial scale.

## Acknowledgments

The authors gratefully acknowledge the financial support from the Jean Barriol Institute from Université de Lorraine.

## References and notes

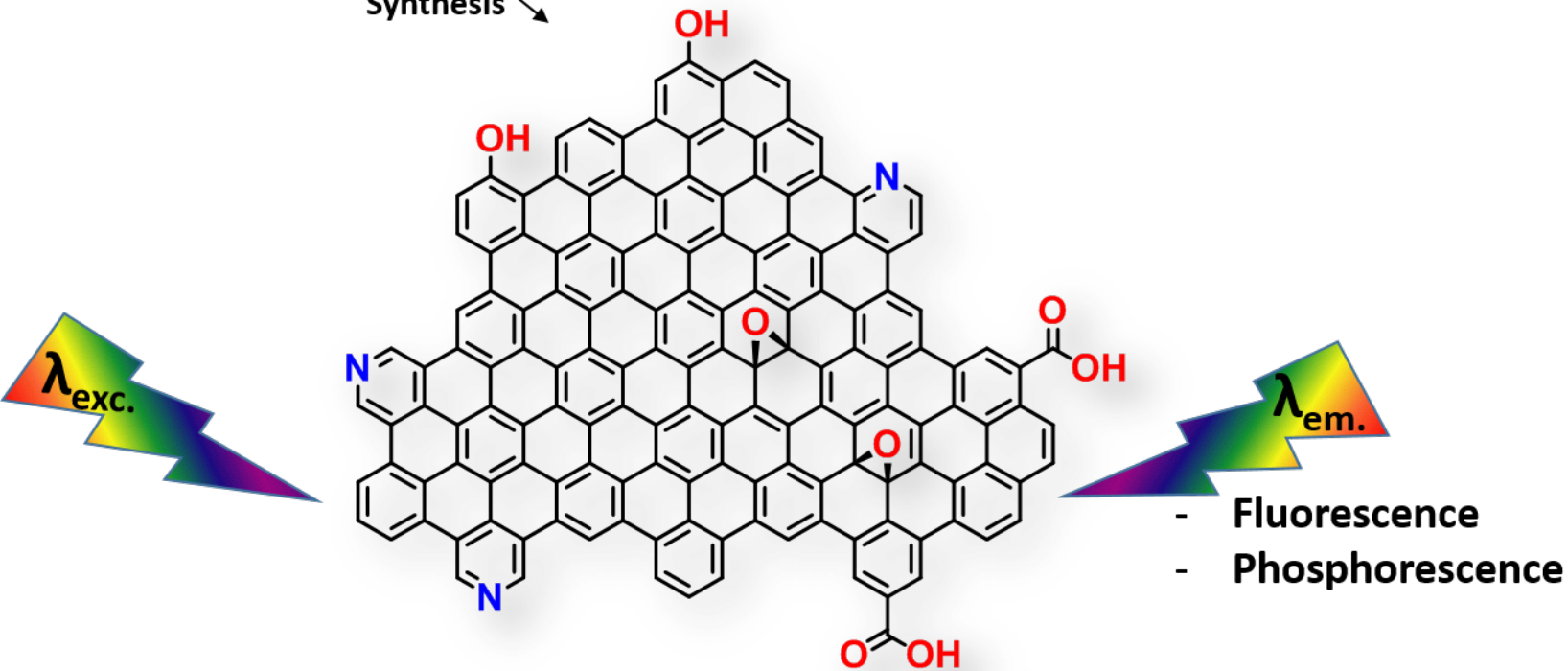
- Xu X, Ray R, Gu Y, Ploehn HJ, Gearheart L, Raker K, Scrivens WA. *Journal of the American Chemical Society*. 2004; 126: 12736–12737.
- Stabel A, Herwig P, Müllen K, Rabe JP. *Angew Chem Int Ed Engl*. 1995; 34: 1609–1611.
- Uno H, Ishiwata M, Muramatsu K, Takase M, Mori S, Okujima T. *BCSJ*. 2019; 92: 973–981.
- Oki K, Takase M, Mori S, Shiotari A, Sugimoto Y, Ohara K, Okujima T, Uno H. *J Am Chem Soc*. 2018; 140: 10430–10434.
- Yokoi H, Hiraoka Y, Hiroto S, Sakamaki D, Seki S, Shinokubo H. *Nat Commun*. 2015; 6: 8215.
- Wei J, Han B, Guo Q, Shi X, Wang W, Wei N. *Angewandte Chemie International Edition*. 2010; 49: 8209–8213.
- Wu D, Pisula W, Haberecht MC, Feng X, Müllen K. *Org Lett*. 2009; 11: 5686–5689.
- Li Q, Zhang S, Dai L, Li L. *J Am Chem Soc*. 2012; 134: 18932–18935.
- Li Q, Zhang S, Dai L, Li L. *J Am Chem Soc*. 2012; 134: 18932–18935.
- Stępień M, Gońka E, Żyła M, Sprutta N. *Chem Rev*. 2017; 117: 3479–3716.
- Yan X, Li B, Li L. *Acc Chem Res*. 2013; 46: 2254–2262.
- Bak S, Kim D, Lee H. *Current Applied Physics*. 2016; 16: 1192–1201.
- Tian P, Tang L, Teng KS, Lau SP. *Materials Today Chemistry*. 2018; 10: 221–258.
- Peng J, Gao W, Gupta BK, Liu Z, Romero-Aburto R, Ge L, Song L, Alemany LB, Zhan X, Gao G, Vithayathil SA, Kaiparettu BA, Marti AA, Hayashi T, Zhu J-J, Ajayan PM. *Nano Lett*. 2012; 12: 844–849.
- Tang D, Liu J, Yan X, Kang L. *RSC Adv*. 2016; 6: 50609–50617.
- Nilewski L, Mendoza K, Jalilov AS, Berka V, Wu G, Sikkema WKA, Metzger A, Ye R, Zhang R, Luong DX, Wang T, McHugh E, Derry PJ, Samuel EL, Kent TA, Tsai A-L, Tour JM. *ACS Appl Mater Interfaces*. 2019; 11: 16815–16821.
- Kaciulis S, Mezzi A, Soltani P, Pizzoferrato R, Ciotta E, Proposito P. *Thin Solid Films*. 2019; 673: 19–25.
- Shen S, Wang J, Wu Z, Du Z, Tang Z, Yang J. *Nanomaterials*. 2020; 10: 375.
- Tian R, Zhong S, Wu J, Jiang W, Shen Y, Jiang W, Wang T. *Optical Materials*. 2016; 60: 204–208.
- Lin J, Huang Y, Wang S, Chen G. *Ind Eng Chem Res*. 2017; 56: 9341–9346.
- Ahirwar S, Mallick S, Bahadur D. *ACS Omega*. 2017; 2: 8343–8353.
- Shin Y, Park J, Hyun D, Yang J, Lee H. *New J Chem*. 2015; 39: 2425–2428.
- Dong Y, Shao J, Chen C, Li H, Wang R, Chi Y, Lin X, Chen G. *Carbon*. 2012; 50: 4738–4743.
- Shehab M, Ebrahim S, Soliman M. *Journal of Luminescence*. 2017; 184: 110–116.
- Wu X, Tian F, Wang W, Chen J, Wu M, Zhao JX. *J Mater Chem C*. 2013; 1: 4676.
- Liu R, Wu D, Feng X, Müllen K. *J Am Chem Soc*. 2011; 133: 15221–15223.
- Qu D, Zheng M, Du P, Zhou Y, Zhang L, Li D, Tan H, Zhao Z, Xie Z, Sun Z. *Nanoscale*. 2013; 5: 12272.

28. Kundu S, Yadav RM, Narayanan TN, Shelke MV, Vajtai R, Ajayan PM, Pillai VK. *Nanoscale*. 2015; 7: 11515–11519.
29. Gao T, Wang X, Yang L-Y, He H, Ba X-X, Zhao J, Jiang F-L, Liu Y. *ACS Appl Mater Interfaces*. 2017; 9: 24846–24856.
30. Sun Y-P, Zhou B, Lin Y, Wang W, Fernando KAS, Pathak P, Mezziani MJ, Harruff BA, Wang X, Wang H, Luo PG, Yang H, Kose ME, Chen B, Veca LM, Xie S-Y. *J Am Chem Soc*. 2006; 128: 7756–7757.
31. Eda G, Lin Y-Y, Mattevi C, Yamaguchi H, Chen H-A, Chen I-S, Chen C-W, Chhowalla M. *Adv Mater*. 2010; 22: 505–509.
32. Baker SN, Baker GA. *Angewandte Chemie International Edition*. 2010; 49: 6726–6744.
33. Jang M-H, Song SH, Ha HD, Seo TS, Jeon S, Cho Y-H. *Carbon*. 2017; 118: 524–530.
34. Zhu S, Shao J, Song Y, Zhao X, Du J, Wang L, Wang H, Zhang K, Zhang J, Yang B. *Nanoscale*. 2015; 7: 7927–7933.
35. Feng Y, Zhao J, Yan X, Tang F, Xue Q. *Carbon*. 2014; 66: 334–339.
36. Jang M-H, Yang H, Chang YH, Park H-C, Park H, Cho HH, Kim BJ, Kim Y-H, Cho Y-H. *Nanoscale*. 2017; 9: 18635–18643.
37. Yeh T-F, Huang W-L, Chung C-J, Chiang I-T, Chen L-C, Chang H-Y, Su W-C, Cheng C, Chen S-J, Teng H. *J Phys Chem Lett*. 2016: 6.
38. Lyu B, Li H-J, Xue F, Sai L, Gui B, Qian D, Wang X, Yang J. *Chemical Engineering Journal*. 2020; 388: 124285.
39. Cao L, Wang X, Mezziani MJ, Lu FS, Wang HF, Luo PJG, Lin Y, Harruff BA, Veca LM, Murray D, Xie SY, Sun YP. *J Am Chem Soc*. 2007; 129: 11318+.
40. Laurenti M, Paez-Perez M, Algarra M, Alonso-Cristobal P, Lopez-Cabarcos E, Mendez-Gonzalez D, Rubio-Retama J. *ACS Appl Mater Interfaces*. 2016; 8: 12644–12651.
41. Singh H, Sreedharan S, Tiwari K, Green NH, Smythe C, Pramanik SK, Thomas JA, Das A. *Chem Commun*. 2019; 55: 521–524.
42. Sekiya R, Uemura Y, Murakami H, Haino T. *Angew Chem Int Ed*. 2014; 53: 5619–5623.
43. Ghosh T, Prasad E. *J Phys Chem C*. 2015; 119: 2733–2742.
44. Li W, Guo H, Li G, Chi Z, Chen H, Wang L, Liu Y, Chen K, Le M, Han Y, Yin L, Vajtai R, Ajayan PM, Weng Y, Wu M. *Nanoscale Horiz*. 2020: 10.1039.D0NH00053A.
45. Deng M, Cao X, Guo L, Cao H, Wen Z, Mao C, Zuo K, Chen X, Yu X, Yuan W. *Dalton Trans*. 2020; 49: 2308–2316.
46. Li Q, Zhou M, Yang M, Yang Q, Zhang Z, Shi J. *Nat Commun*. 2018; 9: 734.
47. Li W, Guo H, Li G, Chi Z, Chen H, Wang L, Liu Y, Chen K, Le M, Han Y, Yin L, Vajtai R, Ajayan PM, Weng Y, Wu M. *Nanoscale Horiz*. 2020: 10.1039.D0NH00053A.
48. Mueller ML, Yan X, McGuire JA, Li L. *Nano Lett*. 2010; 10: 2679–2682.
49. Deng Y, Zhao D, Chen X, Wang F, Song H, Shen D. *Chem Commun*. 2013; 49: 5751.
50. Joseph J, Anappara AA. *ChemistrySelect*. 2017; 2: 4058–4062.
51. Bai LQ, Xue N, Wang XR, Shi WY, Lu C. *Nanoscale*. 2017; 9: 6658–6664.
52. Green DC, Holden MA, Levenstein MA, Zhang S, Johnson BRG, Gala de Pablo J, Ward A, Botchway SW, Meldrum FC. *Nat Commun*. 2019; 10: 206.
53. Long P, Feng Y, Cao C, Li Y, Han J, Li S, Peng C, Li Z, Feng W. *Adv Funct Mater*. 2018; 28: 1800791.
54. Jiang K, Gao X, Feng X, Wang Y, Li Z, Lin H. *Angew Chem Int Ed*. 2020; 59: 1263–1269.
55. Wang C, Chen Y, Xu Y, Ran G, He Y, Song Q. *ACS Appl Mater Interfaces*. 2020; 12: 10791–10800.

Stepwise  
Organic  
Synthesis

Bottom-up

Top-down



**Graphene Quantum Dots  
(GQDs)**